Colloids and Surfaces C: Environmental Aspects 2 (2024) 100025

Contents lists available at ScienceDirect

Colloids and Surfaces C: Environmental Aspects

journal homepage: www.journals.elsevier.com/colloids-and-surfaces-c-environmental-aspects

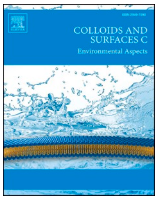

Insights on the synthesis of iron-oxide nanoparticles and the detection of iron-reducing genes from soil microbes

Oluwafemi Bamidele Daramola [a,*], Reama Chinedu George [b], Nkem Torimiro [a], Afusat Ajoke Olajide [b]

[a] Department of Microbiology, Obafemi Awolowo University, Ile-Ife 220005, Nigeria
[b] Department of Chemistry, Obafemi Awolowo University, Ile-Ife 220005, Nigeria

ARTICLE INFO

Keywords:
Iron oxide nanoparticles
Klebsiella species
Bacillus species
Iron tolerance
Iron reductase
Cysteine desulfurase

ABSTRACT

This study explores the potential of some soil bacteria in the synthesis of iron oxide nanoparticles (IONPs), highlighting their advantages in terms of iron uptake and tolerance capacity. Soil samples collected from a metal fabricating workshop were successively screened in nutrient broth containing 1% iron salts (Fe_2O_3, $FeCl_3$, and $FeSO_4$) following a standard microbiological sampling technique. The recovered bacterial isolates (persister cells) were identified using polymerase chain reaction (PCR) and 16S rRNA sequencing. Ten bacterial isolates identified as *Sporosarcina luteola, Bacillus badius* (2), *Bacillus subtilis* (2), *Bacillus tropicus, Bacillus cereus, Klebsiella pneumoniae, Klebsiella quasipneumoniae* and *Klebsiella africana* were recovered. The method reports that six of the bacterial isolates extracellularly synthesize IONPs and the result from the energy dispersion x-ray (EDX) spectral analysis indicated varying weight percentages of bio-reduced iron by *Bacillus subtilis*-A12 (48.59%), *Klebsiella quasipneumoniae* (39.99%), *Bacillus subtilis*-B1 (39.97%), *Bacillus cereus* (38.62%), *Bacillus badius* (33.79%) and *Klebsiella africana* (32.61%). The IONPs exhibited absorbance peaks in the range of 250–350 nm, with a mean area size estimated between 31–72 nm using ImageJ software. Additionally, the presence of iron reductase (*fhu*) and cysteine desulfurase (*suf*) genes were detected in the recovered *Bacillus* and *Klebsiella* species through PCR analysis. This study has provided valuable insights into the physiology and genomic functions essential for microbial synthesis of IONPs and their relevance to nano-bioremediation.

1. Introduction

Several approaches have been reported under chemical and physical methods for the production of metal and noble-metal nanoparticles, but the emergence of the biological approach otherwise known as “green synthesis or biosynthesis” has paved the way with enormous interest regarding its application [1]. This technique using various biological entities across the world and their optimization processes has emerged as a rapid research approach, producing quick, stable, and desirable morphologies and sizes for wider application [2–4]. The biosynthesis method of nanoparticles provides several advantages which include clean, non-toxic, and eco-friendly procedures when compared to both physical and chemical methods [5]. They also reduce the high production cost of nanoparticles and eliminate harmful processes required in physical and chemical synthesis [6].

As a branch of biological approach, microbes and their bio-molecules have been found relevant in the synthesis of nanoparticles [7]. Most importantly, the establishment of microbial enzymes as useful biomolecules responsible for the bio-reduction of bulk metal compounds into their respective nanoparticles [8,9]. Reports have shown that different biochemical and molecular mechanisms in many microbes are essential for the biosynthesis of nanoparticles both intracellularly and extracellularly [5,10]. The deposition of these enzymes which were utilized for the production of relatively pure nanoparticles is of utmost advantage including the ability to pattern the production and assemblage of nanoparticles into stabilized robust structures [11,12].

Microbial synthesis of iron oxide nanoparticles (IONPs) using iron as a precursor via the metabolic activities of magnetotactic and iron-reducing bacteria has been reported [13–16]. Iron oxide and magnetic nanoparticles produced from iron salts have gained attention in studies and widespread applications, especially for medical purposes due to their magnetic properties [17–19]. Iron oxide nanoparticles have been reported to exist as hematite (α-Fe_2O_3), maghemite (γ-Fe_2O_3), and magnetite (Fe_3O_4) [20]. Some reported studies have established the

---

* Corresponding author.
E-mail address: oluwafemidaramola8@gmail.com (O.B. Daramola).

https://doi.org/10.1016/j.colsuc.2023.100025
Received 24 August 2023; Received in revised form 21 November 2023; Accepted 23 November 2023

potential of some bacteria possessing varying ferric reductases required for the bio-reduction of iron salts. They include *Agrobacterium tumefaciens, Azotobacter vinelandii, Bacillus megaterium, Bacillus subtilis, Escherichia coli, Legionella pneumophila, Listeria monocytogenes, Magnetospirillum magnetotacticum, Vibrio vulnificus, Magnetospirillum gryphiswaldense, Mycobacterium paratuberculosis, Mycobacterium smegmatis, Neisseria gonorrhoeae, Pseudomonas putida, Pseudomonas aeruginosa, Pseudomonas fluorescens, Rhodopseudomonas sphaeroides,* and *Treponema denticola* [21–23]. An earlier study by Vadas *et al.* [24] described the identification and characterization of a novel ferric reductase from a hyperthermophilic Archaeon –*Archaeoglobus fulgidus*, revealing its ability to bio-reduce iron for assimilation and to complement the microbe cellular protein. Sedláček *et al.* [25], in their study, identified ferric reductase subunit A as an essential enzyme for effective iron acquisition in *Paracoccus denitrificans*. In another related study, Shinagawa [26] established the presence of Fe(III)-EDTA reductase from *Bacillus* sp. B-3 through purification and characterization of the identified enzyme.

Depending on the bacterial species and the mechanism of iron bioreduction/uptake, ferric reductases have been identified in several locations within microbial cells namely, cytoplasmic and periplasmic membranes. These membrane-bound locations have been reported in *Spirillum itersoni*, *Escherichia coli,* and *Staphylococcus aureus* [21]. As documented in research, ferric reductases are often produced in a culture medium due to the presence of surface-bound ferric reductases in most groups of microorganisms [27]. In some cases, microbes secrete metabolic intermediates such as citrate and specially synthesized siderophores (low molecular mass molecules) to chelate ferric iron for easy reduction and cellular uptake activity of iron in their cell [28,29].

Despite the promising mechanism in the bio-reduction of iron salts and the synthesis of iron oxide nanoparticles by some bacterial species as reported in studies aforementioned, there is a paucity of studies in recent times reporting on the potential of new microbes capable of bioreducing, and the uptake of iron salts alongside their iron tolerance level during the synthesis of IONPs. In addition, there has been little to no study reporting the detection of iron-reducing genes and how they are essential genetic material responsible for the production of enzymes required in the synthesis of iron oxide nanoparticles. Hence this study sought to report the bio-reduction and uptake of iron salts potential of some indigenous bacteria isolated in a metal fabricating workshop in Nigeria, detect some underreported iron-reducing genes and their relevance in the production of iron oxide nanoparticles.

2. Methods

2.1. Screening and isolation of bacteria from the soil sample

Soil samples from the Center for Technological Laboratory and Workshop (CTLW) (7°30’39"N; 4 °31’31" E), a metal fabricating workshop in Obafemi Awolowo University, Ile-Ife was collected. Soil sample about 5 cm below the surface was collected in sterile sample bottles for the isolation of bacteria. The modified method of Elcey *et al.* [30] was used for the screening. Five grams of the soil sample was weighed and transferred into 45 mL nutrient broth containing 1% iron salts of Fe_2O_3, $FeCl_3$, and $FeSO_4$ (Sigma Aldrich, United Kingdom) respectively. The inoculated flasks were incubated at 37 °C for 48 h after which 0.1 mL from each flask was spread-plated on nutrient agar and incubated at 37 °C for 18–24 h. To further screen and recover only persistent bacterial cells, freshly prepared nutrient broths containing each of the iron salts (1% w/v) were inoculated with 5 mL of the previously cultured broths. The flasks were incubated at 37 °C for 48 h. Thereafter, 0.1 mL from the flasks were spread-plated on nutrient agar and incubated at 37 °C for 18–24 h. Growth observed from the cultured plates for the first and second screening flasks were re-subcultured by the streaking method to obtain pure colonies of the bacterial isolates. The pure bacterial isolates recovered were subjected to Gram- and endospore staining tests [31].

2.2. Molecular identification of bacterial isolates using 16S rRNA sequencing

The identities of the bacterial isolates were determined using polymerase chain reaction (PCR) and 16S rRNA sequencing techniques. Pure colonies of the bacterial cultures were re-subcultured in nutrient broth at 37 °C for 18–24 h. About 500 μL of the sub-cultured cells were dispensed in Eppendorf tubes, centrifuged at 6000 rpm for 5 min, and the culture broth discarded. The cells were re-suspended in 400 μL sterile nuclease-free water (Bioconcept, Switzerland), vortexed, and subjected to the heat lysis method [32]. The tubes were placed in heat blocks and boiled at 100 °C for 10 min, transferred in the freezer (−20 °C) for 5 min. The suspension was centrifuged at 10,000 rpm for 5 min and the supernatant was kept in the freezer (4 °C) for further analysis. The Polymerase chain reaction (PCR) cocktail was prepared using supplied reagents which include 2X OneTaq Quick-Load PCR Master Mix (New England Biolabs, United Kingdom), universal oligonucleotides for bacteria (Forward “CCAGCAGCCGCGGTAATACG”; Reverse “ATCGGCTACCTTGTTACGACTTC”) prepared to 10 μM working concentration and nuclease-free water. Thereafter, 25 μL final volume was prepared in 200 μL PCR tubes for a single reaction of each bacterial isolate to include master mix (12.5 μL); forward primer (1 μL); reverse primer (1 μL); nuclease-free water (5.5 μL) and DNA template (5 μL) [33].

The reaction was performed in an automated thermal cycler, GeneAmp PCR System 9700 (Applied Biosystems, USA) under the following optimized cycling program: an initial denaturation step at 94 °C for 4 min; 30 cycles of denaturation at 94 °C for 30 s, annealing at 53 °C for 1 min, extension at 68 °C for 2 min; and a final extension at 68 °C for 5 min. The temperature was maintained at 4 °C for further use. The amplified PCR fragments were analyzed using ethidium bromide (5 μL) stained 1.2% agarose gel submerged in 0.5X Tris-Boric Acid-EDTA (TBE) buffer. Both the amplified PCR products and DNA 100 bp marker-loaded wells were subjected to an electrophoresis condition of 135 V for 20 min. Gel images were visualized under UV illumination by comparing them with the DNA 100 bp marker. Aligning amplified PCR fragments were sequenced and analyzed using the basic local alignment search tool (BLAST). The resulting sequences were aligned with the most similar bacterial species found in the GenBank (https://www.ncbi.nlm.nih.gov/Blast.cgi). The evolutionary histories of the bacterial isolates were inferred by using the maximum likelihood method and the Tamura 3-parameter model. The evolutionary analyses were conducted with MEGA X software [34].

2.3. Microbial synthesis of iron oxide nanoparticles using culture supernatant

About 50 mL of sterile nutrient broth prepared in conical flasks were inoculated with bacterial isolates. Inoculated flasks incubated at 37 °C for 48 h were centrifuged at 3000 rpm for 10 min and the culture supernatants were transferred into cell-free conical flasks. The synthesis method previously described was used for this experiment [35]. A cocktail of 1 mM $FeCl_3$ and $FeSO_4$; 50 mM $FeCl_3$ and $FeSO_4$ were prepared in flasks to a final volume of 15 mL respectively. The culture supernatants of the bacterial isolates (20 mL) were added to the two iron cocktails and allowed to stand at room temperature (25 °C) for 5 days. The electronic spectra and functional groups of the synthesis solution were analyzed using UV-Vis spectrophotometer-1800 (Shimadzu, Japan) and Fourier Transform Infrared Spectroscopy (FT-IR, Agilent Technologies, USA) scanned between 200 and 700 nm and 4000 – 500 cm^{-1} respectively.

To obtain solid samples of IONPs, the crude product was centrifuged at 10,000X g for 10 min. While the supernatant fluid was decanted, the precipitate was washed thrice with sterile distilled water. A slight adjustment was considered for the temperature condition as reported by Omole *et al.* [36] for the recovery of the dried particles. Colloidal solutions were oven-dried at 120 °C for 60 min using a sterile glass Petri plate. The dried particles were analyzed and characterized by scanning electron microscope (SEM, JSM-6390LV Jeol, Japan), and energy dispersive x-ray (EDX, 6733B–1UUS Thermo Electron Corporation, USA) to determine the particle sizes, shapes, and elemental composition of the samples respectively [37,38].

2.4. Iron uptake and tolerance of bacterial isolates

Modified Dailey standard method as described by Sasaki *et al.* [39] and Bharde *et al.* [10] was used for iron uptake and tolerance, assessing both the microbial cell and culture supernatant respectively. To assess iron uptake and tolerance screening from bacterial culture supernatant, a cocktail of $FeCl_3$ and $FeSO_4$ (1 mM and 50 mM) was prepared in 100 mL conical flasks to a final volume of 40 mL respectively. The reaction was initiated by introducing 10 mL of 48 h-old bacterial culture supernatants. Flasks were placed in an incubating shaker (100 rpm/30 ± 2 °C) for 9 days and 1 mL samples were taken at the 24 h interval. Withdrawn samples were mixed with 0.5 mL ethylenediaminetetraacetic acid (EDTA), an iron chelator, and allowed to stand for 30–45 min. The spectral measurement was done using a UV-Vis spectrophotometer (Jenway, United Kingdom) at 562 nm [10]. For the microbial cell screening, a cocktail of $FeCl_3$ and $FeSO_4$ (1 mM and 50 mM) were prepared in conical flasks to a final volume of 40 mL containing 1.5% NaCl. The reaction was initiated by introducing 10 mL of bacterial wet biomass. Flasks were placed in an incubating shaker (100 rpm/30 ± 2 °C) for 7 days and 1 mL samples were taken at the 24 h interval. Withdrawn samples were mixed with 0.5 mL iron chelator (EDTA) and allowed to stand for 30–45 min. The spectral measurement was done using a UV-Vis spectrophotometer at 562 nm [39].

2.5. Molecular detection of iron reductase and cysteine desulfurase genes from iron oxide nanoparticles synthesizing bacteria

Iron reductase (*fhuA, fhuD*) and cysteine desulfurase (*sufB, sufD*) oligonucleotides were specifically designed for the identified bacterial isolates using relevant bioinformatics databases and software in this study. Complete genomes and annotations of the best-match species obtained from the 16 S rRNA sequences blast were downloaded from the National Center for Biotechnology Information (https://www.ncbi.nlm.nih.gov). Iron reductase and cysteine desulfurase housekeeping genes were isolated using Artemis (version 17.0.1). Sequences' similarities were checked using the Artemis comparison tool (version 17.0.1) and MegaX. Oligonucleotides were designed and validated using Primer3-plus and NCBI primer designing tool (https://www.ncbi.nlm.nih.gov/tools/primer-blast) respectively. The oligonucleotides were sourced from Inqaba Biotechnical Industries (Pty) Ltd (South Africa). Oligonucleotides comprising iron reductase (*fhuA, fhuD*) and cysteine desulfurase (*sufB, sufD*) genes targeting some of the molecularly identified bacteria namely, *Klebsiella* and *Bacillus* species were screened for the iron-reducing (ferric reductase) genes (Table 1). The molecular method of detection as described in Section 2.3 was also used for the detection of these iron-reducing genes.

2.6. Statistical analysis

The absorbance reading data obtained were subjected to exponential smoothening and plotted as scattered lines on Microsoft Excel (Microsoft Office 2019). Evolutionary analyses of the bacterial isolates were presented as a phylogenetic tree using MegaX software. ImageJ software was used to analyze the average particle sizes and shapes.

3. Results and discussion

The screening result revealed a slight to a visible change in the color of the 1% iron salts. This was most evident for Fe_2O_3 salt with a color change from reddish-brown to black after 48 h of incubation. During the screening process, bacterial growth was observed in both the initial and subsequent screening stages of broths containing Fe_2O_3 and $FeSO_4$ iron salts. However, no bacterial isolate was recovered during the second successive screening stage involving $FeCl_3$ salt. Blast hits of the bacterial isolate sequences recovered from the first and second screening stage were identified as *Sporosarcina luteola* (A1)*, Bacillus badius* (A2, A11)*, Bacillus subtilis* (A12, B1)*, Bacillus cereus* (B2)*, Bacillus tropicus* (C2)*, Klebsiella pneumoniae* (C1)*, Klebsiella africana* (C11) and *Klebsiella quasipneumoniae* (C12). The phylogenetic relatedness of the recovered bacteria isolates is also displayed in Fig. 1.

The bacterial isolates investigated in this study are widely distributed in the environment and can colonize a wide range of ecological niches. These bacteria species can exhibit different growth patterns, which is mostly determined by their inherent genetic characteristics required for adaptability and survival [40] depending on the environment these bacteria are found. Although many environmental stresses, such as radiation, nutrient scarcity, extreme temperatures, and desiccation, pose challenges limiting bacteria survival and metabolic activities in the natural environment [41]. In the natural environment, the metabolism of carbon and nitrogen contributes to these bacteria's ability to thrive in diverse environments [42]. However, this study showed that iron derivatives in trace amounts could also be an alternative nutritional requirement for their survival in the natural environment with nutrient scarcity or devoid of primary growth requirements. These bacteria most importantly, *Bacillus* and *Klebsiella* species as reported in this study often adapt readily to various available nutrients in their environment by expressing genes that would support the metabolic activity of the available nutrient. According to Cain and Smith [43], iron naturally appears to be in the ferric (Fe^{3+}) oxidation state in the presence of O_2, and thus, very reactive in aqueous environments, prompting its sequestration into cofactors and their host proteins to remain soluble. In addressing this, many unicellular pathogens release siderophores, which are high-affinity Fe^{3+} chelators with low molecular weight [44]. This is necessary to initiate the needed metabolic pathways and in the process of hydrolyzing the siderophore backbone to liberate the chelated Fe^{3+}.

Among the three iron salts, $FeCl_3$ exhibits the highest propensity for generating ROS, making it the most toxic to organisms [45]. However, $FeCl_3$ is less commonly found in natural soil environments, unlike Fe_2O_3 and $FeSO_4$, which occur more naturally. Fe_2O_3, commonly known as rust, is likely the most prevalent iron compound in the workshop. Given its usage in the mentioned workshop, the presence of $FeCl_3$ poses a

Table 1
Primer sequences used for the detection of *Iron Reductase* and *Cysteine Desulfurase* genes in bacterial isolates.

Gene code		Primer sequence (5′– 3′)	Target	Annealing temp. (°C)	Product size (bp)
fhuA	F	AGAAGAAACTATCACCGTCG	*Iron reductase (subunit A)* in *Klebsiella* spp	46	338
	R	CAGAGTAGTTATTCCCCTGC			
fhuD	F	ATATTCCCAACTATCGCTT	*Iron reductase (subunit D)* in *Klebsiella* spp	39	399
	R	TTTCGCCAAACACCA			
sufD	F	GCTATCACTTCGCCCATAA	*Cysteine desulfurase (Subunit D)* in *Klebsiella* spp	46	338
	R	GAGCAGCAGATTATTGTTGG			
sufB	F	TGCCGTTATACAACGATCCA	*Cysteine desulfurase (Subunit B)* in *Bacillus* spp	45	250
	R	ATGTGTTTGGTGCAAGGTGA			

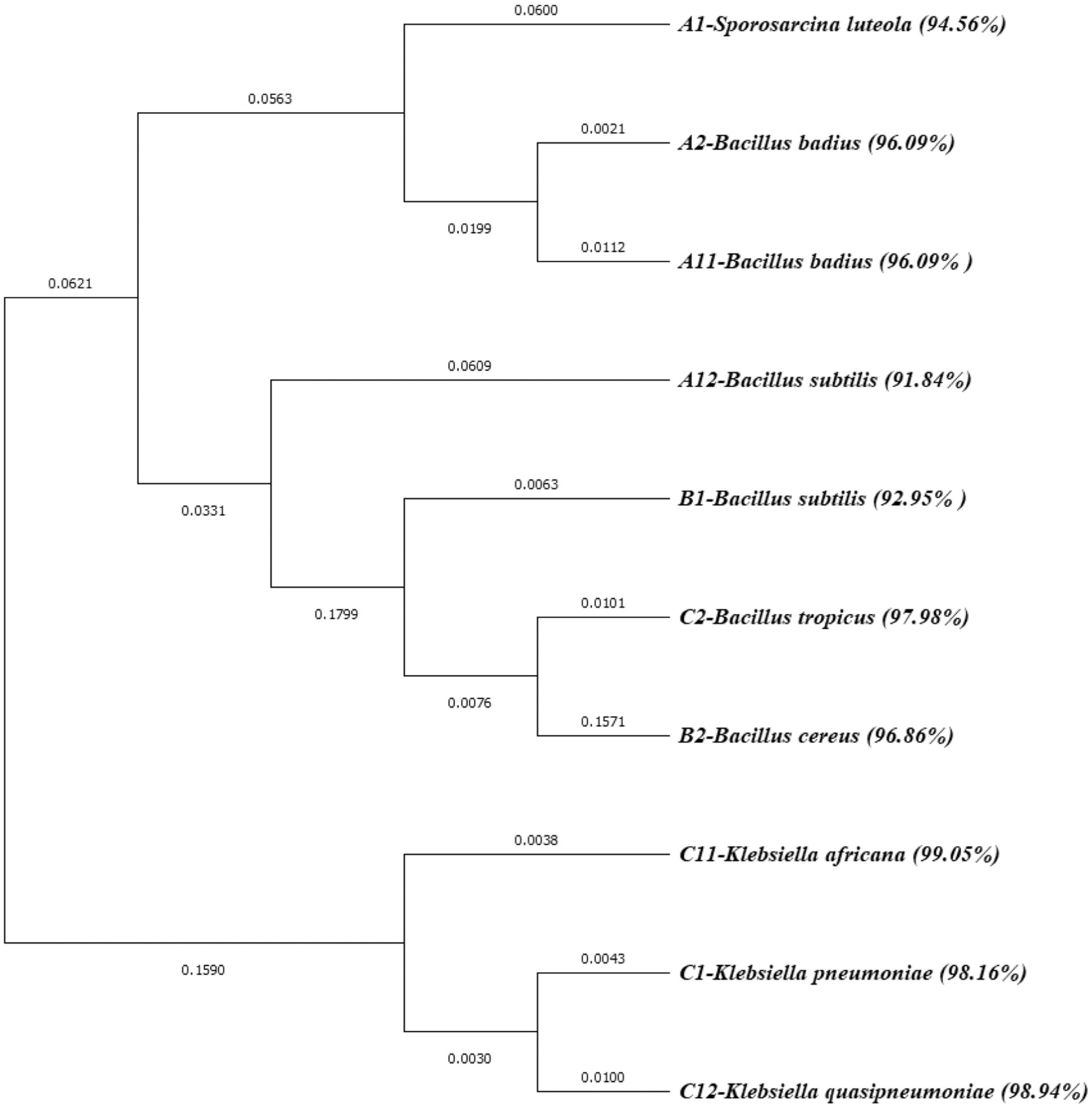

Fig. 1. Phylogenetic tree of the bacterial strains isolated from the soil samples.

challenge to the survival of organisms, as they may not possess the necessary adaptations to tolerate its toxic effects. Similarly, the indiscriminate release of $FeCl_3$ into the natural environment may also pose some challenges to bacteria community diversity and survival. The pollution of the environment by $FeCl_3$ and other toxic contaminants may impede bacteria-mediated short- and long-term bioremediation and degradation activities relevant to ecological restoration.

The crude product from the synthesis of the IONPs were white colloidal suspensions with black and brown precipitate for 1 mM and 50 mM iron cocktails. Based on the UV-Vis absorption spectra depicted in Fig. 2, it was noted that both concentrations of the iron cocktails exhibited a λ_{max} around 400 nm. However, when the bacterial isolates were subjected to bio-reduction, the intensity of this band decreased, and a new band emerged within the 250–350 nm range which is the surface plasmon resonances as specified for iron oxide nanoparticles [2,3,19]. Regarding the 1 mM concentration sample, *Klebsiella quasipneumoniae* (C12) displayed the highest absorbance among the isolates, whereas *Bacillus subtilis* (A12) exhibited the lowest absorbance. In contrast, for the 50 mM concentration of the cocktail, the absorbance of *Bacillus badius* (A11), *Klebsiella africana* (C11), and *Klebsiella quasipneumoniae* (C12) decreased compared to the parameters of the 1 mM cocktail synthesis. However, there was an increase in absorbance values for *Bacillus subtilis* (A12, B1), and *Bacillus cereus* (B2) at both the 1 mM and 50 mM concentrations.

It is noteworthy to mention that to the best of our knowledge, this would be the first report on the ability of *Klebsiella africana, Klebsiella quasipneumoniae*, and *Bacillus badius to* synthesize IONPs. Several studies have reported the synthesis of iron oxide nanoparticles from both Gram-

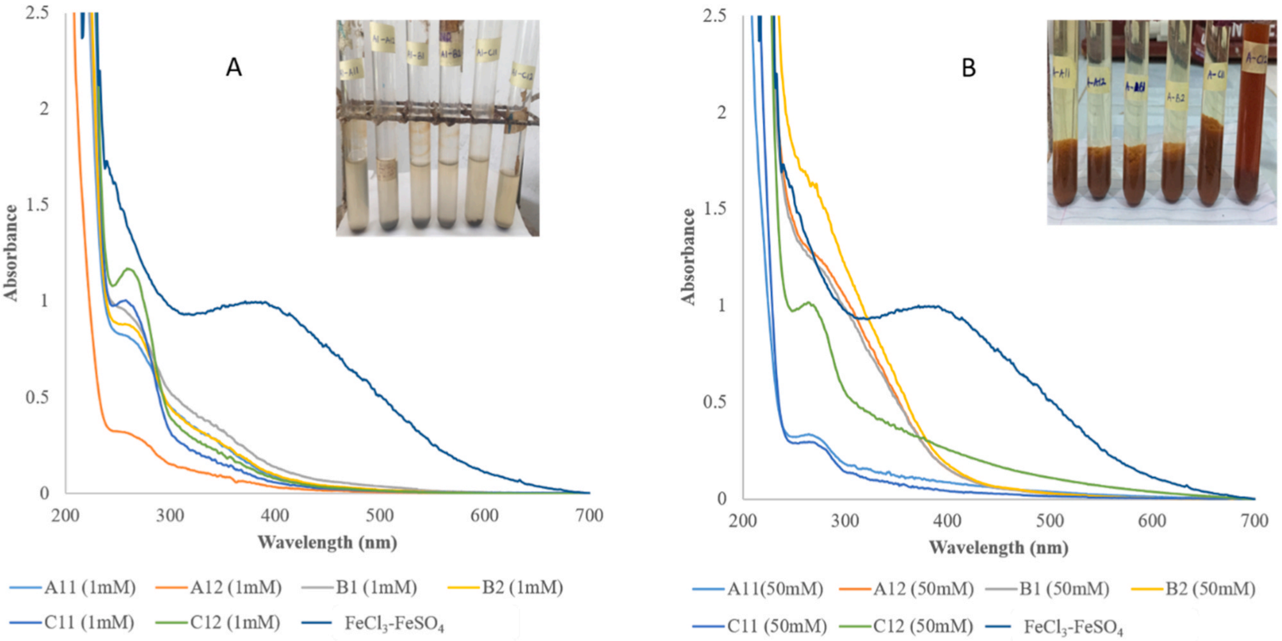

UV spectra of IONPs synthesis from $FeCl_3$ and $FeSO_4$ cocktail (1mM) by bacterial isolates (culture supernatant)

(Inset: colorimetric change in tubes)

UV spectra of IONPs synthesis from $FeCl_3$ and $FeSO_4$ cocktail (50mM) by bacterial isolates (culture supernatant)

(Inset: colorimetric change in tubes)

Fig. 2. UV-Vis spectra of iron oxide nanoparticles.

positive bacteria such as *Bacillus subtilis* [46], *Bacillus megaterium* [47], and Gram-negative bacteria such as *Proteus vulgaris* [48], *Pseudomonas aeruginosa* [49], *Escherichia coli* [50].

The FT-IR interpretation analyses for the identification of the functional groups revealed several numbers of detectable peaks. Four spectral peaks representing intermolecular bonded O-H stretch of alcohol, N-H bend of amine, skeletal C-C stretch vibration, and aliphatic C-Cl stretch were identified in *Bacillus subtilis* (A12), *Bacillus cereus* (B2) and *Klebsiella africana* (C11) while other bacterial isolates namely, *Bacillus badius* (A11), *Bacillus subtilis* (B1), and *Klebsiella quasipneumoniae* (C12) showed lesser spectral peaks as shown in Fig. 3. The functional groups reported in this study have also been documented in the microbial synthesis of iron oxide nanoparticles [46,48,51]. The ability of bacteria in this study to synthesize iron oxide nanoparticles could be attributed to the presence of primary components responsible for the release of some biomolecules. According to studies, these biomolecules which include

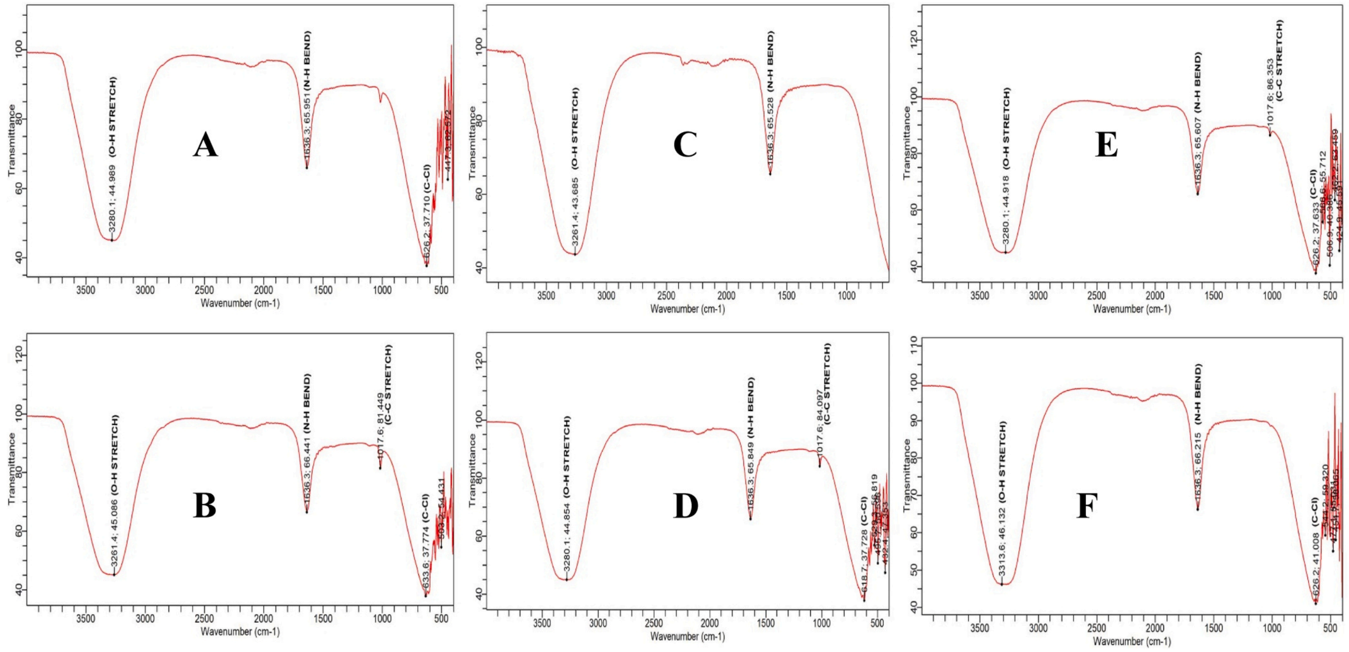

Fig. 3. FT-IR Spectral peaks in IONPs colloidal solution synthesized by *Bacillus badius*-A11 (A), *Bacillus subtilis*-A12 (B), *Bacillus subtilis* -B1 (C), *Bacillus cereus*-B2 (D), *Klebsiella africana* -C11 (E) and *Klebsiella quasipneumoniae* -C12 (F).

enzymes (NADPH-dependent nitrate reductases, iron reductases), steroids, carbohydrates, proteins, amino acids, flavonoids, tannins, saponins, alkaloids, exopolysaccharides (EPS), and cell wall components (alginate, laminarian) could be vital in the bio-reduction, stabilization and capping of metals [51,52]. This could have increased their capability of tolerating and bio-reducing high iron salt concentration in the environment, although, may vary among bacterial cells.

The SEM images (Fig. 4) of the iron oxide nanoparticles showed that they were flaky and highly poly-dispersed with a mean area size ranging from 31 to 72 nm and within the purview of its classification as nanomaterials [53]. Narayanan and Sakthivel [54] and Prodan *et al.* [55] documented that microbial incubation (biological method) could synthesize different shapes and morphology such as spherical, rod, and irregular spheres depending on the synthesis condition. The elemental composition as displayed by the EDX quantification result revealed the presence and varying weight (%) of iron (Fig. 5). The peaks around 0.7 keV are related to the binding energies of Fe, alongside the peak of oxygen at 0.5 keV and this confirmed the presence of both iron and oxygen in the synthesized NPs and also similar to peaks documented by Rahman *et al.* [56]. The weight percentage of zero-valent iron present in each sample showed *Bacillus subtilis* with the highest zero-valent iron weight percentage. The presence of other elements was also observed representing carbon, sodium, nitrogen, aluminum, silicon, phosphorus, potassium, calcium, and chlorine. It is assumed that these elements are metabolites released by these bacterial isolates [57–59]. The Cl and S peaks are mostly from the $FeSO_4$ and $FeCl_3$ precursors used as part of the cocktail salts in the synthesis of these nanoparticles.

Iron tolerance and bio-reduction were different for each condition (Fig. 6). The presence of metabolites in the supernatant and released metabolites by the wet biomass confirms the extracellular synthesis of IONPs in the solution [60–62]. Sample A (1 mM cocktail plus the supernatant) was the only one with a steady increase in uptake and increase in metabolite tolerance and activities as the days progressed except for *B1* (*Bacillus subtilis*) which exhibited a decrease by Day 6 (Fig. 6a). At an increased concentration, Sample B (50 mM of the iron salts cocktail), the extracellular metabolites in the cell-free filtrates exhibited low tolerance (Fig. 6b). In the other samples (Sample C and D -wet biomass) no bio-reduction or significant uptake of iron salts by microbial cells intracellular metabolites were observed as compared to extracellular metabolites. A few exceptions did occur but at low concentrations; in Sample C (1 mM cocktail) there was a fluctuating increase and decrease in uptake by *Bacillus subtilis*, (B1) and *Bacillus badius* (A11) (Fig. 6c, insert). *Klebsiella quasipneumoniae* (C12) in Sample D (50 mM cocktail) showed a slightly increased uptake by Day 5 and then decreased by Day 6 (Fig. 6d, insert).

Bacterial ferric reductases investigated in this study are soluble proteins that are either exclusive to certain forms of ferric iron complexes or have a broad spectrum of activity [63,64]. In line with this, many bacteria in soil possess ferric reductase enzymes derived from proteins located in the cytoplasmic membrane [65–67]. These studies have shown that these reductases transport reducing equivalents from cytosolic reductants over the lipid bilayer, either into the periplasmic membrane or the extracellular area. It also gives an indication that the iron-dependent enzymes taking part in the bio-reduction of iron salts are often released extracellularly in culture medium and not bio-reduced intracellularly as observed for bacterial isolates in this study. Several studies support the extracellular bio-reduction of iron salts whose method involves the use of reducing enzymes from several locations within bacterial cell membranes which include a periplasmic membrane [1,68]. Here the assessment on the bio-reduction of iron salts by viable cells enzymatic activity indicates a conventional metabolic release of iron-reducing enzyme in the growth medium, and that, trace/small concentrations of iron salts are best and can be efficiently bio-reduced by most bacterial culture medium-ladened with essential enzymes and

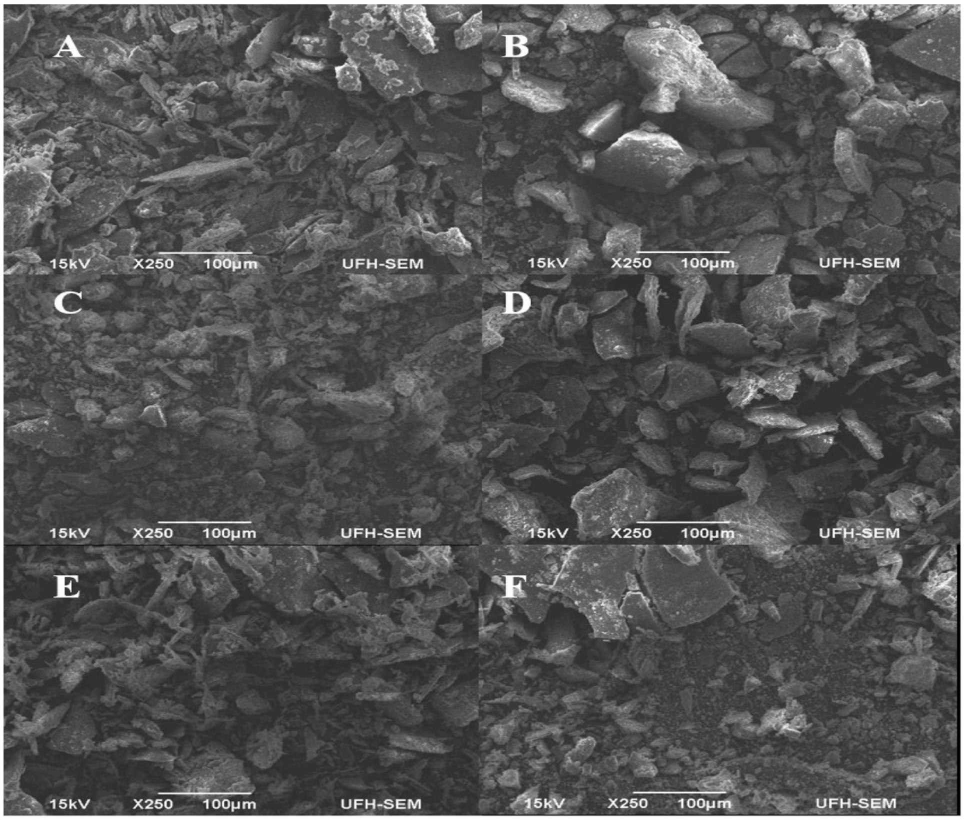

Fig. 4. Scanning electron microscope images of dried iron oxide nanoparticles produced from bacterial isolates (*Bacillus badius*-A11 (A), *Bacillus subtilis*-A12 (B), *Bacillus subtilis* -B1 (C), *Bacillus cereus*-B2 (D), *Klebsiella africana* -C11 (E) and *Klebsiella quasipneumoniae* -C12 (F)).

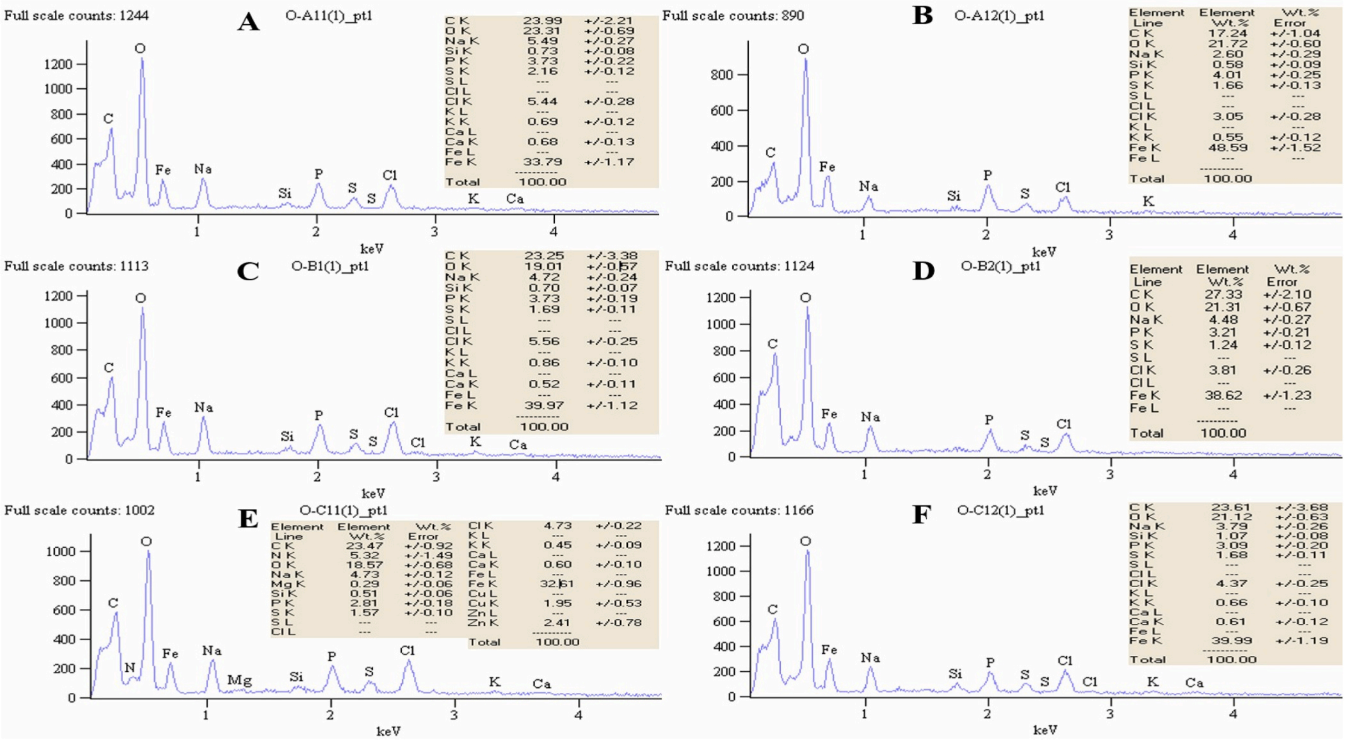

A

Element Line	Element Wt.%	Wt.% Error
C K	23.99	+/-2.21
O K	23.31	+/-0.69
Na K	5.49	+/-0.27
Si K	0.73	+/-0.08
P K	3.73	+/-0.22
S K	2.16	+/-0.12
S L	---	---
Cl L	---	---
Cl K	5.44	+/-0.28
K L	---	---
K K	0.69	+/-0.12
Ca L	---	---
Ca K	0.68	+/-0.13
Fe L	---	---
Fe K	33.79	+/-1.17
Total	100.00	

B

Element Line	Element Wt.%	Wt.% Error
C K	17.24	+/-1.04
O K	21.72	+/-0.60
Na K	2.60	+/-0.29
Si K	0.58	+/-0.09
P K	4.01	+/-0.25
S K	1.66	+/-0.13
S L	---	---
Cl L	---	---
Cl K	3.05	+/-0.28
K L	---	---
K K	0.55	+/-0.12
Fe K	48.59	+/-1.52
Fe L	---	---
Total	100.00	

C

Element Line	Element Wt.%	Wt.% Error
C K	23.25	+/-3.38
O K	19.01	+/-0.57
Na K	4.72	+/-0.24
Si K	0.70	+/-0.07
P K	3.73	+/-0.19
S K	1.69	+/-0.11
S L	---	---
Cl L	---	---
Cl K	5.56	+/-0.25
K L	---	---
K K	0.86	+/-0.10
Ca L	---	---
Ca K	0.52	+/-0.11
Fe L	---	---
Fe K	39.97	+/-1.12
Total	100.00	

D

Element Line	Element Wt.%	Wt.% Error
C K	27.33	+/-2.10
O K	21.31	+/-0.67
Na K	4.48	+/-0.27
P K	3.21	+/-0.21
S K	1.24	+/-0.12
S L	---	---
Cl K	3.81	+/-0.26
Cl L	---	---
Fe K	38.62	+/-1.23
Fe L	---	---
Total	100.00	

E

Element Line	Element Wt.%	Wt.% Error
C K	23.47	+/-0.92
N K	5.32	+/-1.49
O K	18.57	+/-0.68
Na K	4.73	+/-0.12
Mg K	0.29	+/-0.06
Si K	0.51	+/-0.06
P K	2.81	+/-0.18
S K	1.57	+/-0.10
S L	---	---
Cl L	---	---
Cl K	4.73	+/-0.22
K L	---	---
K K	0.45	+/-0.09
Ca L	---	---
Ca K	0.60	+/-0.10
Fe L	---	---
Fe K	32.61	+/-0.96
Cu L	---	---
Cu K	1.95	+/-0.53
Zn L	---	---
Zn K	2.41	+/-0.78
Total	100.00	

F

Element Line	Element Wt.%	Wt.% Error
C K	23.61	+/-3.68
O K	21.12	+/-0.63
Na K	3.79	+/-0.26
Si K	1.07	+/-0.08
P K	3.09	+/-0.20
S K	1.68	+/-0.11
S L	---	---
Cl L	---	---
Cl K	4.37	+/-0.25
K L	---	---
K K	0.66	+/-0.10
Ca L	---	---
Ca K	0.61	+/-0.12
Fe L	---	---
Fe K	39.99	+/-1.19
Total	100.00	

Fig. 5. Energy dispersive X-ray of dried iron oxide nanoparticles produced from bacterial isolates (*Bacillus badius*-A11 (A), *Bacillus subtilis*-A12 (B), *Bacillus subtilis* -B1 (C), *Bacillus cereus*-B2 (D), *Klebsiella africana* -C11 (E) and *Klebsiella quasipneumoniae* -C12 (F)).

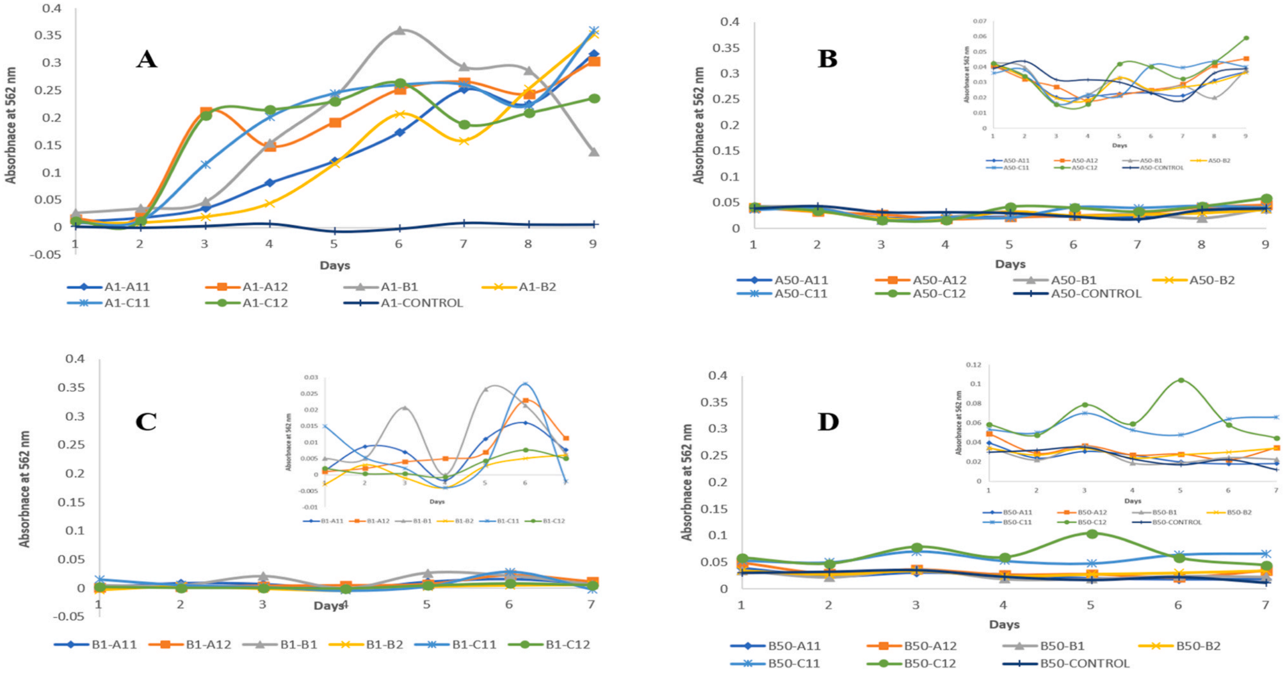

Fig. 6. Iron tolerance of bacterial culture supernatant and cells to $FeCl_3$ and $FeSO_4$ Cocktail (A= ImM cocktail and supernatant; B= 50 mM cocktail and supernatant; C= 1 mM cocktail and wet biomass; D = 50 mM and wet biomass).

metabolites useful for the bio-reduction activity [69,70].

This study further corroborates the location of iron reductase enzymes required for bio-reduction of iron salts in microbial cells as it tends to be prominent at the cellular region hence, facilitating its action and immediate release into the growth medium [71]. This study showed that, for the microbial synthesis of extracellular IONPs, many parameters such as the type of bacteria used as bio-reducing agents, the volume of metabolites released by the bacteria, duration of reaction, and environmental conditions (such as incubating temperature) played a significant role in the size, shape, surface charge and reactivity of the formed NPs.

The presence of iron reductase and cysteine desulfurase subunit genes were found in *Klebsiella* and *Bacillus* genome isolates. *Iron reductase subunit A* (*fhuA*) was detected in *Klebsiella pneumoniae* (C1), *Klebsiella africana* (C11), and *Klebsiella quasipneumoniae* (C12) while *iron reductase subunit D* (*fhuD*) were present in *Klebsiella pneumoniae* (C1), and *Klebsiella quasipneumoniae* (C12) (Fig. 7a and b). *Cysteine desulfurase subunit D* (*sufD)* was confirmed in the 3 *Klebsiella* spp (*Klebsiella pneumoniae* (C1), *Klebsiella africana* (C11) and *Klebsiella quasipneumoniae* (C12)) as presented in Fig. 8. Similarly, oligonucleotides designed for *Bacillus* spp in this study confirmed the presence of *cysteine desulfurase subunit B* (*sufB)* genes in all *Bacillus* spp isolated for the study (Fig. 9). It was observed that the *Klebsiella* species possess the *fhuA*. However, reports have shown that the gene is more pronounced in *E. coli* [72–74]. Nevertheless, it has been observed to perform the same function in the uptake of iron in a complex with ferrichrome, a hydroxamate-type siderophore, which binds and transports ferrichrome iron across the outer membrane [75]. The primer sequence first reported in this research could be relevant for the detection of the *fhuA* gene in most *Klebsiella* species. The *FhuD* gene was detected in *K. pneumoniae* and *K. quasipneumoniae*. Similar to *fhuA*, *fhuD* has also received extensive confirmation in *E. coli* [76,77]. It functions mainly in binding Fe^{3+}-hydroxamate complex and transferring the same to the membrane-bound permease hence, often required for the transport of all Fe^{3+}-hydroxamate siderophores such as ferrichrome aiding iron uptake in bacteria cells [78]. The bio-reduction of iron salts by *Klebsiella* culture supernatant observed in our study indicates the release of iron reductase protein from the bacteria periplasmic membrane into the supernatant by the *fhuD* gene.

This was suggested and deemed possible in that, *fhuD* protein contains a typical signal sequence of 30 amino acids at the amino terminus which displays characteristics of a soluble protein, that may be exported into the periplasm [79].

Cysteine desulfurase (*Suf*) gene has been documented as an important protein that contributes to the assembly or repair of oxygen-labile iron-sulfur clusters under oxidative stress and could also facilitate iron uptake from extracellular iron chelators under iron limitation [80]. Iron-sulfur clusters which include cysteine desulfurase (*suf*) remain the oldest, ubiquitous, indispensable, and most versatile inorganic cofactors that are required to sustain fundamental life processes [81,82]. Earlier studies have reported *sufB* and *sufD* in *Bacillus subtilis* [83] and other bacteria such as *E. coli* [84,85], and *Enterococcus faecalis* [86], hence, its detection in *Bacillus* and *Klebsiella* isolates in this work suggest these genes are essential for the biogenesis of Fe-S cluster in the *SufBCD* complex [87]. The presence of iron reductase and cysteine desulfurase subunit genes among environmental *Klebsiella* and *Bacillus* species isolated in this study showed that these genes play significant functional roles in the natural synthesis of iron oxide nanoparticles via the bio-reduction and metabolism of bulky iron materials that could be present in the environment. This further suggests that soil bacteria encoding iron-reducing genes in the environment are relevant and essential in maintaining the required amount of iron on the earth's surface to ensure a sustainable environment.

Microbially synthesis of IONPs has some advantages in the eco-restoration of the environment. These include treatment and remediation of heavy metals, hydrocarbons, dyes and other pollutants in wastewater [7,88]. The low production cost, large specific surface area and enhanced reactivity of IONPs increase their adsorption properties and allow for more efficient removal of a wide range of contaminants in the environment [89,90]. The magnetic properties of IONPs also enable easy magnetic separation of pollutants from the environment. However, its limitations to the environment are in its tendency to agglomerate and react quickly with oxygen and water, leading to the formation of iron oxides that may decrease treatment and remediation efficiency [91]. The formation of iron oxides such as superparamagnetic iron nanoparticles (SPION) may also induce some toxicity to soil microbes, soil invertebrates, aquatic life and human health [92,93].

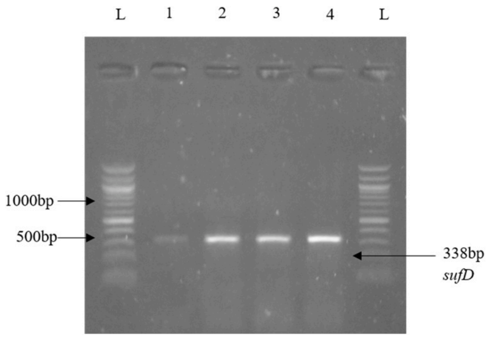

Fig. 8. The detection of cysteine desulfurase subunit *D (sufD)* Gene in *Klebsiella* spp.

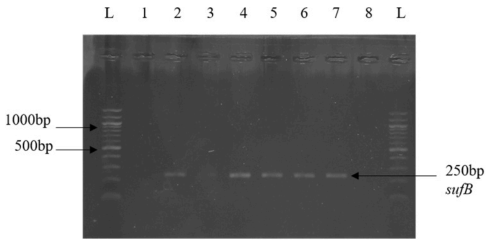

Fig. 9. The detection of cysteine desulfurase subunit B *(sufB)* Gene in *Bacillus* spp.

4. Conclusion

Our study reports on new species of *Klebsiella* and *Bacillus* and their iron uptake ability. In addition, the result established the importance of iron for bacterial growth, proliferation and survival. The bacterial isolates obtained from the second successive screening stage proved that they are promising bio-reducing agents useful for the synthesis of iron oxide NPs from iron(III) chloride and ferrous sulfate cocktail precursors. This study further supported the preference for biological (green) especially microbial synthesis methods over thermal, electrochemical, and chemical methods of synthesis. Our findings equally revealed that iron uptake, bio-reduction and tolerance levels vary in each bacterial

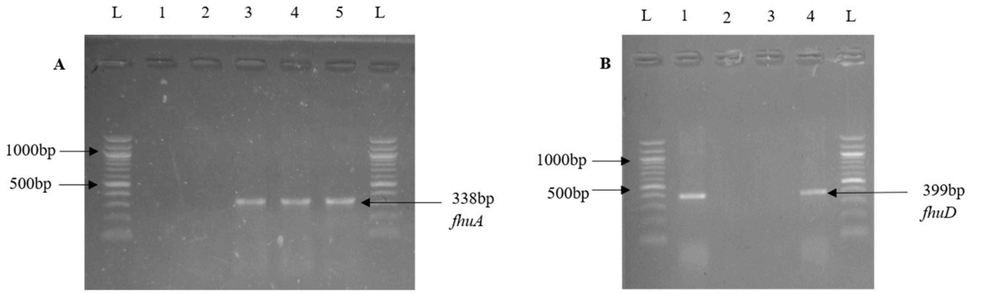

Fig. 7. The detection of iron reductase subunit A *(fhuA)* (A) and subunit D *(fhuD)* (B) Genes in *Klebsiella* spp.

isolate taking into consideration the concentration of iron salts, and the incubating condition. In all, our research work has provided some important details on the physiological and genomics functional abilities and potentials of the *Bacillus* and *Klebsiella* species as promising bacterial isolates relevant to the microbial synthesis of iron oxide nanoparticles. This study has laid some emphasis on the importance of iron metabolism which could facilitate IONPs synthesis and support nano-bioremediation in the environment.

Funding

This research work was supported by the West African Research Association and MasterCard Foundation (Ideas Matter Fellowship Award, 2021 awarded to Oluwafemi Daramola). The supporting foundation had no role in the study's design, data analysis and decision to publish.

CRediT authorship contribution statement

Oluwafemi B. Daramola: Conceptualization, Methodology, Formal Analysis, Data Curation, Data Visualization, Writing – Original Draft, Writing - Review & Editing; **Reama C. George:** Supervision, Methodology, Data Validation, Writing - Review & Editing; **Nkem Torimiro:** Supervision, Data Validation, Writing - Review & Editing; **Afusat A. Olajide:** Data Validation, Writing - Review & Editing.

Declaration of Competing Interest

The authors declare the following financial interests/personal relationships which may be considered as potential competing interests: Oluwafemi Bamidele Daramola reports financial support was provided by Boston University West African Research Association.

Acknowledgments

The authors appreciate Dr. Taiwo Fadare for the provided help during the research.

Appendix A. Supporting information

Supplementary data associated with this article can be found in the online version at doi:10.1016/j.colsuc.2023.100025.

References

[1] P. Singh, Y.-J. Kim, D. Zhang, D.-C. Yang, Biological synthesis of nanoparticles from plants and microorganisms, Trends Biotechnol. 34 (2016) 588–599, https://doi.org/10.1016/j.tibtech.2016.02.006.

[2] M. Nadeem, R. Khan, N. Shah, I.R. Bangash, B.H. Abbasi, C. Hano, C. Liu, S. Ullah, S.S. Hashmi, A. Nadhman, J. Celli, A review of microbial mediated iron nanoparticles (IONPs) and Its biomedical applications, Nanomater. 12 (2021) 130, https://doi.org/10.3390/nano12010130.

[3] S. Eshghi, F. Jookar Kashi, Bacterial synthesis of magnetic Fe3O4 nanoparticles: decolorization acid red 88 using FeNPs/Ca-Alg beads, Arab. J. Chem. 15 (2022), 104032, https://doi.org/10.1016/j.arabjc.2022.104032.

[4] O.B. Daramola, R.K. Omole, I.V. Akinwale, F.O. Otuyelu, B.A. Akinsanola, T. O. Fadare, R.C. George, N. Torimiro, Bio-receptors functionalized nanoparticles: a resourceful sensing and colorimetric detection tool for pathogenic bacteria and microbial biomolecules, Front. Nanotechnol. 4 (2022), 885803, https://doi.org/10.3389/fnano.2022.885803.

[5] F. Ramezani, M. Ramezani, S. Talebi, Mechanistic aspects of biosynthesis of nanoparticles by several microbes, Nanocon 10 (2010) 1–7.

[6] S.K. Dorcheh, K. Vahabi, Biosynthesis of nanoparticles by fungi: large-scale production, in: J.-M. Mérillon, K.G. Ramawat (Eds.), Fungal Metabolites, Springer International Publishing, Cham, 2016, pp. 1–20, https://doi.org/10.1007/978-3-319-19456-1_8-1.

[7] N. Torimiro, O.B. Daramola, O.D. Oshibanjo, F.O. Otuyelu, B.A. Akinsanola, O. O. Yusuf, O.T. Ore, R.K. Omole, Ecorestoration of heavy metals and toxic chemicals in polluted environment using microbe-mediated nanomaterials, Int. J. Environ. Bioremediat. Biodegrad. 9 (2021) 8–21, https://doi.org/10.12691/ijebb-9-1-2.

[8] D.S. Balaji, S. Basavaraja, R. Deshpande, D.B. Mahesh, B.K. Prabhakar, A. Venkataraman, Extracellular biosynthesis of functionalized silver nanoparticles by strains of Cladosporium cladosporioides fungus, Colloids Surf. B Biointerfaces 68 (2009) 88–92, https://doi.org/10.1016/j.colsurfb.2008.09.022.

[9] N. Saifuddin, C.W. Wong, A.A.N. Yasumira, Rapid biosynthesis of silver nanoparticles using culture supernatant of bacteria with microwave irradiation, E J. Chem. 6 (2009) 61–70, https://doi.org/10.1155/2009/734264.

[10] A.A. Bharde, R.Y. Parikh, M. Baidakova, S. Jouen, B. Hannoyer, T. Enoki, B.L. V. Prasad, Y.S. Shouche, S. Ogale, M. Sastry, Bacteria-mediated precursor-dependent biosynthesis of superparamagnetic iron oxide and iron sulfide nanoparticles, Langmuir 24 (2008) 5787–5794, https://doi.org/10.1021/la704019p.

[11] B. Calderon, A. Fullana, Heavy metal release due to aging effect during zero valent iron nanoparticles remediation, Water Res. 83 (2015) 1–9, https://doi.org/10.1016/j.watres.2015.06.004.

[12] D.K. Tripathi, V.P. Singh, S.M. Prasad, D.K. Chauhan, N.K. Dubey, Silicon nanoparticles (SiNp) alleviate chromium (VI) phytotoxicity in Pisum sativum (L.) seedlings, Plant Physiol. Biochem. 96 (2015) 189–198, https://doi.org/10.1016/j.plaphy.2015.07.026.

[13] D.A. Bazylinski, R.B. Frankel, Magnetosome formation in prokaryotes, Nat. Rev. Microbiol. 2 (2004) 217–230, https://doi.org/10.1038/nrmicro842.

[14] H. Vali, B. Weiss, Y.-L. Li, S.K. Sears, S.S. Kim, J.L. Kirschvink, C.L. Zhang, Formation of tabular single-domain magnetite induced by Geobacter metallireducens GS-15, Proc. Natl. Acad. Sci. 101 (2004) 16121–16126, https://doi.org/10.1073/pnas.0404040101.

[15] A. Scheffel, M. Gruska, D. Faivre, A. Linaroudis, J.M. Plitzko, D. Schüler, An acidic protein aligns magnetosomes along a filamentous structure in magnetotactic bacteria, Nature 440 (2006) 110–114, https://doi.org/10.1038/nature04382.

[16] M.A.-A. Elblbesy, A.K. Madbouly, T.A.-A. Hamdan, Bio-synthesis of magnetite nanoparticles by bacteria, Am. J. Nano Res. Appl. 2 (2014) 98, https://doi.org/10.11648/j.nano.20140205.12.

[17] T.T. Hien Pham, C. Cao, S.J. Sim, Application of citrate-stabilized gold-coated ferric oxide composite nanoparticles for biological separations, J. Magn. Magn. Mater. 320 (2008) 2049–2055, https://doi.org/10.1016/j.jmmm.2008.03.015.

[18] S.A. Ansari, M. Oves, R. Satar, A. Khan, S.I. Ahmad, M.A. Jafri, S.K. Zaidi, M. H. Alqahtani, Antibacterial activity of iron oxide nanoparticles synthesized by co-precipitation technology against and, Pol. J. Chem. Technol. 19 (2017) 110–115, https://doi.org/10.1515/pjct-2017-0076.

[19] F. Batool, M.S. Iqbal, S.-U.-D. Khan, J. Khan, B. Ahmed, M.I. Qadir, Biologically synthesized iron nanoparticles (FeNPs) from Phoenix dactylifera have anti-bacterial activities, Sci. Rep. 11 (2021) 22132, https://doi.org/10.1038/s41598-021-01374-4.

[20] M. Coduri, P. Masala, L. Del Bianco, F. Spizzo, D. Ceresoli, C. Castellano, S. Cappelli, C. Oliva, S. Checchia, M. Allieta, D.-V. Szabo, S. Schlabach, M. Hagelstein, C. Ferrero, M. Scavini, Local structure and magnetism of Fe2O3 maghemite nanocrystals: the role of crystal dimension, Nanomaterials 10 (2020) 867, https://doi.org/10.3390/nano10050867.

[21] I. Schröder, E. Johnson, S. De Vries, Microbial ferric iron reductases, FEMS Microbiol. Rev. 27 (2003) 427–447, https://doi.org/10.1016/S0168-6445(03)00043-3.

[22] J. Yeom, C.O. Jeon, E.L. Madsen, W. Park, Ferredoxin-NADP+ reductase from Pseudomonas putida functions as a ferric reductase, J. Bacteriol. 191 (2009) 1472–1479, https://doi.org/10.1128/JB.01473-08.

[23] C. Zhang, X. Meng, N. Li, W. Wang, Y. Sun, W. Jiang, G. Guan, Y. Li, Two bifunctional enzymes with ferric reduction ability play complementary roles during magnetosome synthesis in Magnetospirillum gryphiswaldense MSR-1, J. Bacteriol. 195 (2013) 876–885, https://doi.org/10.1128/JB.01750-12.

[24] A. Vadas, H.G. Monbouquette, E. Johnson, I. Schröder, Identification and characterization of a novel ferric reductase from the hyperthermophilic Archaeon Archaeoglobus fulgidus *, J. Biol. Chem. 274 (1999) 36715–36721, https://doi.org/10.1074/jbc.274.51.36715.

[25] V. Sedláček, R.J.M. van Spanning, I. Kučera, Ferric reductase A is essential for effective iron acquisition in Paracoccus denitrificans, Microbiology 155 (2009) 1294–1301, https://doi.org/10.1099/mic.0.022715-0.

[26] E. Shinagawa, Purification and characterization of Fe(III)-EDTA reductase from Bacillus sp. B-3, Biosci. Biotechnol. Biochem 75 (2011) 2063–2065, https://doi.org/10.1271/bbb.110397.

[27] V. Braun, M. Braun, Active transport of iron and siderophore antibiotics, Curr. Opin. Microbiol. 5 (2002) 194–201, https://doi.org/10.1016/s1369-5274(02)00298-9.

[28] J.H. Crosa, C.T. Walsh, Genetics and assembly line enzymology of siderophore biosynthesis in bacteria, Microbiol Mol. Biol. Rev. 66 (2002) 223–249, https://doi.org/10.1128/MMBR.66.2.223-249.2002.

[29] P. Visca, L. Leoni, M.J. Wilson, I.L. Lamont, Iron transport and regulation, cell signalling and genomics: lessons from Escherichia coli and Pseudomonas, Mol. Microbiol 45 (2002) 1177–1190, https://doi.org/10.1046/j.1365-2958.2002.03088.x.

[30] C.D. Elcey, A.T. Kuruvilla, D. Thomas, Synthesisof magnetite nanoparticles from optimized iron reducing bacteria isolated fromiron ore mining sites, J. Mater. Environ. Sci. 3 (2014) 408–417.

[31] C. Shen, Y. Zhang, Staining technology and bright-field microscope use, in: C. Shen, Y. Zhang (Eds.), Food Microbiology Laboratory for the Food Science Student: A Practical Approach, Springer International Publishing, Cham, 2023, pp. 9–17, https://doi.org/10.1007/978-3-031-26197-8_2.

[32] J. Yamagishi, Y. Sato, N. Shinozaki, B. Ye, A. Tsuboi, M. Nagasaki, R. Yamashita, Comparison of boiling and robotics automation method in DNA extraction for metagenomic sequencing of human oral microbes, e0154389, PLoS One 11 (2016), https://doi.org/10.1371/journal.pone.0154389.

[33] J.-J. Lu, C.-L. Perng, S.-Y. Lee, C.-C. Wan, Use of PCR with universal primers and restriction endonuclease digestions for detection and identification of common bacterial pathogens in cerebrospinal fluid, J. Clin. Microbiol. 38 (2000) 2076, https://doi.org/10.1128/jcm.38.6.2076-2080.2000.

[34] S. Kumar, G. Stecher, M. Li, C. Knyaz, K. Tamura, MEGA X: molecular evolutionary genetics analysis across computing platforms, Mol. Biol. Evol. 35 (2018) 1547–1549, https://doi.org/10.1093/molbev/msy096.

[35] K.R. Abhilash, B.D. Pandey, Microbial synthesis of iron-based nanomaterials—a review, Bull. Mater. Sci. 34 (2011) 191–198, https://doi.org/10.1007/s12034-011-0076-6.

[36] R.K. Omole, N. Torimiro, S.O. Alayande, E. Ajenifuja, Silver nanoparticles synthesized from Bacillus subtilis for detection of deterioration in the post-harvest spoilage of fruit, Sustain. Chem. Pharm. 10 (2018) 33–40, https://doi.org/10.1016/j.scp.2018.08.005.

[37] W.B. Ayinde, M. Gitari, M. Muchindu, A. Samie, Biosynthesis of ultrasonically modified Ag-MgO nanocomposite and its potential for antimicrobial activity, J. Nanotechnol. (2018), https://doi.org/10.1155/2018/9537454.

[38] G.M. Sulaiman, A.T. Tawfeeq, A.S. Naji, Biosynthesis, characterization of magnetic iron oxide nanoparticles and evaluations of the cytotoxicity and DNA damage of human breast carcinoma cell lines, Artif. Cells Nanomed. Biotechnol. 46 (2018) 1215–1229, https://doi.org/10.1080/21691401.2017.1366335.

[39] T. Sasaki, N. Kurano, S. Miyachi, Induction of ferric reductase activity and of iron uptake capacity in chlorococcum littorale cells under extremely High-CO$_2$ and iron-deficient conditions, Plant Cell Physiol. 39 (1998) 405–410, https://doi.org/10.1093/oxfordjournals.pcp.a029383.

[40] S. Diomande, C. Nguyen-The, M.-H. Guinebretière, V. Broussolle, J. Brillard, Role of fatty acids in Bacillus environmental adaptation, Front. Microbiol. 6 (2015). 〈https://www.frontiersin.org/articles/10.3389/fmicb.2015.00813〉 (accessed November 8, 2023).

[41] A. Deng, T. Wang, J. Wang, L. Li, X. Wang, L. Liu, T. Wen, Adaptive mechanisms of Bacillus to near space extreme environments, Sci. Total Environ. 886 (2023), 163952, https://doi.org/10.1016/j.scitotenv.2023.163952.

[42] C. Blin, V. Passet, M. Touchon, E.P.C. Rocha, S. Brisse, Metabolic diversity of the emerging pathogenic lineages of Klebsiella pneumoniae, Environ. Microbiol. 19 (2017) 1881–1898, https://doi.org/10.1111/1462-2920.13689.

[43] T.J. Cain, A.T. Smith, Ferric iron reductases and their contribution to unicellular ferrous iron uptake, J. Inorg. Biochem. 218 (2021), 111407, https://doi.org/10.1016/j.jinorgbio.2021.111407.

[44] E.R. Frawley, F.C. Fang, The Ins and Outs of bacterial iron metabolism, Mol. Microbiol. 93 (2014) 609–616, https://doi.org/10.1111/mmi.12709.

[45] S.J. Dixon, B.R. Stockwell, The role of iron and reactive oxygen species in cell death, Nat. Chem. Biol. 10 (2014) 9–17, https://doi.org/10.1038/nchembio.1416.

[46] S. Khan, N. Akhtar, S.U. Rehman, S. Shujah, E.S. Rha, M. Jamil, Bacillus subtilis synthesized iron oxide nanoparticles (Fe3O4 NPs) induced metabolic and anti-oxidative response in rice (Oryza sativa L.) under arsenic stress, Toxics 10 (2022) 618, https://doi.org/10.3390/toxics10100618.

[47] S. Hajiali, S. Daneshjou, S. Daneshjoo, Biomimetic synthesis of iron oxide nanoparticles from Bacillus megaterium to be used in hyperthermia therapy, AMB Expr. 12 (2022) 1–11, https://doi.org/10.1186/s13568-022-01490-y.

[48] S. Majeed, M. Danish, M.N. Mohamad Ibrahim, S.H. Sekeri, M.T. Ansari, A. Nanda, G. Ahmad, Bacteria mediated synthesis of iron oxide nanoparticles and their antibacterial, antioxidant, cytocompatibility properties, J. Clust. Sci. 32 (2021) 1083–1094, https://doi.org/10.1007/s10876-020-01876-7.

[49] A.A. Khan, S. Khan, S. Khan, S. Rentschler, S. Laufer, H.-P. Deigner, Biosynthesis of iron oxide magnetic nanoparticles using clinically isolated Pseudomonas aeruginosa, Sci. Rep. 11 (2021) 20503, https://doi.org/10.1038/s41598-021-99814-8.

[50] J.H. Jung, M. Cho, T.S. Seo, S.Y. Lee, Biosynthesis and applications of iron oxide nanocomposites synthesized by recombinant Escherichia coli, Appl. Microbiol. Biotechnol. 106 (2022) 1127–1137, https://doi.org/10.1007/s00253-022-11779-4.

[51] M.J. Jacinto, V.C. Silva, D.M.S. Valladão, R.S. Souto, Biosynthesis of magnetic iron oxide nanoparticles: a review, Biotechnol. Lett. 43 (2021) 1–12, https://doi.org/10.1007/s10529-020-03047-0.

[52] F.S. Al-khattaf, Gold and silver nanoparticles: green synthesis, microbes, mechanism, factors, plant disease management and environmental risks, Saudi J. Biol. Sci. 28 (2021) 3624–3631, https://doi.org/10.1016/j.sjbs.2021.03.078.

[53] O.B. Daramola, N. Torimiro, S.O. Alayande, Affinity capture of Escherichia coli pathotypes using poly-L-lysine functionalized silver nanoparticles, Adv. Nat. Sci. Nanosci. Nanotechnol. 13 (2022), 025012, https://doi.org/10.1088/2043-6262/ac7712.

[54] K.B. Narayanan, N. Sakthivel, Biological synthesis of metal nanoparticles by microbes, Adv. Colloid Interface Sci. 156 (2010) 1–13, https://doi.org/10.1016/j.cis.2010.02.001.

[55] A.M. Prodan, S.L. Iconaru, C.S. Ciobanu, M.C. Chifiriuc, M. Stoicea, D. Predoi, Iron oxide magnetic nanoparticles: characterization and toxicity evaluation by In Vitro and In Vivo assays, J. Nanomater. 2013 (2013), e587021, https://doi.org/10.1155/2013/587021.

[56] S.S.U. Rahman, M.T. Qureshi, K. Sultana, W. Rehman, M.Y. Khan, M.H. Asif, M. Farooq, N. Sultana, Single step growth of iron oxide nanoparticles and their use as glucose biosensor, Results Phys. 7 (2017) 4451–4456, https://doi.org/10.1016/j.rinp.2017.11.001.

[57] S.M. Mortazavi, M. Khatami, I. Sharifi, H. Heli, K. Kaykavousi, M.H. Sobhani Poor, S. Kharazi, M.A.L. Nobre, Bacterial biosynthesis of gold nanoparticles using Salmonella enterica subsp. enterica serovar Typhi Isolated from blood and stool specimens of patients, J. Clust. Sci. 28 (2017) 2997–3007, https://doi.org/10.1007/s10876-017-1267-0.

[58] P. Pourali, S.H. Badiee, S. Manafi, T. Noorani, A. Rezaei, B. Yahyaei, Biosynthesis of gold nanoparticles by two bacterial and fungal strains, Bacillus cereus and Fusarium oxysporum, and assessment and comparison of their nanotoxicity in vitro by direct and indirect assays, Electron. J. Biotechnol. 29 (2017) 86–93, https://doi.org/10.1016/j.ejbt.2017.07.005.

[59] M.P. Patil, J.-O. Kim, Y.B. Seo, M. Kang, G.-D. Kim, Biogenic synthesis of metallic nanoparticles and their antibacterial applications, J Life Sci. 31 (2021) 862–872, https://doi.org/10.5352/JLS.2021.31.9.862.

[60] H. Bahrulolum, S. Nooraei, N. Javanshir, H. Tarrahimofrad, V.S. Mirbagheri, A. J. Easton, G. Ahmadian, Green synthesis of metal nanoparticles using microorganisms and their application in the agrifood sector, J. Nanobiotechnology 19 (2021) 86, https://doi.org/10.1186/s12951-021-00834-3.

[61] B. Koul, A.K. Poonia, D. Yadav, J.-O. Jin, Microbe-mediated biosynthesis of nanoparticles: applications and future prospects, Biomolecules 11 (2021) 886, https://doi.org/10.3390/biom11060886.

[62] M. Benković, D. Valinger, T. Jurina, J. Gajdoš Kljusurić, A. Jurinjak Tušek, Biocatalysis as a green approach for synthesis of iron nanoparticles—batch and microflow process comparison, Catalysts 13 (2023) 112, https://doi.org/10.3390/catal13010112.

[63] M. Miethke, A.J. Pierik, F. Peuckert, A. Seubert, M.A. Marahiel, Identification and characterization of a novel-type ferric siderophore reductase from a gram-positive extremophile, J. Biol. Chem. 286 (2011) 2245–2260, https://doi.org/10.1074/jbc.M110.192468.

[64] K. Li, W.-H. Chen, S.-D. Bruner, Structure and mechanism of the Siderophore-interacting protein from the Fuscachelin gene cluster of Thermobifida fusca, Biochemistry 54 (2015), https://doi.org/10.1021/acs.biochem.5b00354.

[65] G. Ganne, K. Brillet, B. Basta, B. Roche, F. Hoegy, V. Gasser, I.J. Schalk, Iron release from the Siderophore Pyoverdine in Pseudomonas aeruginosa involves three new actors: FpvC, FpvG, and FpvH, ACS Chem. Biol. 12 (2017) 1056–1065, https://doi.org/10.1021/acschembio.6b01077.

[66] E.D. Peng, S.M. Payne, Vibrio cholerae VciB mediates iron reduction, e00874-16, J. Bacteriol. 199 (2017), https://doi.org/10.1128/JB.00874-16.

[67] F.M. Arnold, M.S. Weber, I. Gonda, M.J. Gallenito, S. Adenau, P. Egloff, I. Zimmermann, C.A.J. Hutter, L.M. Hürlimann, E.E. Peters, J. Piel, G. Meloni, O. Medalia, M.A. Seeger, The ABC exporter IrtAB imports and reduces mycobacterial siderophores, Nature 580 (2020) 413–417, https://doi.org/10.1038/s41586-020-2136-9.

[68] K. Punjabi, S. Mehta, S. Yedurkar, R. Jain, S. Mukherjee, A. Kale, S. Deshpande, Extracellularsynthesis of silver nanoparticle by *Pseudomonas hibiscicola* –Mechanistic approach, Adv. Nano Res. 1 (6) (2018) 81–92.

[69] S.C. Andrews, A.K. Robinson, F. Rodríguez-Quiñones, Bacterial iron homeostasis, FEMS Microbiol. Rev. 27 (2003) 215–237, https://doi.org/10.1016/S0168-6445(03)00055-X.

[70] B.J. Kim, J.H. Park, T.H. Park, P.A. Bronstein, D.J. Schneider, S.W. Cartinhour, M. L. Shuler, Effect of Iron concentration on the growth rate of Pseudomonas syringae and the expression of virulence factors in hrp-inducing minimal medium, Appl. Environ. Microbiol. 75 (2009) 2720–2726, https://doi.org/10.1128/AEM.02738-08.

[71] Y. Lan, M. Zhou, X. Li, X. Liu, J. Li, W. Liu, Preliminary investigation of iron acquisition in hypervirulent Klebsiella pneumoniae mediated by outer membrane vesicles, IDR 15 (2022) 311–320, https://doi.org/10.2147/IDR.S342368.

[72] X. Chen, X. Cai, Z. Chen, J. Wu, G. Hao, Q. Luo, S. Liu, J. Zhang, Y. Hu, G. Zhu, W. Koester, A.P. White, Y. Cai, Y. Wang, Mosaic evolution of beta-barrel-porin-encoding genes in Escherichia coli, e0006022, Appl. Environ. Microbiol. 88 (2022), https://doi.org/10.1128/aem.00060-22.

[73] C.L. Pocanschi, J.H. Kleinschmidt, The thermodynamic stability of membrane proteins in micelles and lipid bilayers investigated with the Ferrichrom receptor FhuA, J. Membr. Biol. 255 (2022) 485–502, https://doi.org/10.1007/s00232-022-00238-w.

[74] Z. Wei, Y. Wei, H. Li, D. Shi, D. Yang, J. Yin, S. Zhou, T. Chen, J. Li, M. Jin, Emerging pollutant metformin in water promotes the development of multiple-antibiotic resistance in Escherichia coli via chromosome mutagenesis, J. Hazard Mater. 430 (2022), 128474, https://doi.org/10.1016/j.jhazmat.2022.128474.

[75] M. Bonhivers, L. Plançon, A. Ghazi, P. Boulanger, M. le Maire, O. Lambert, J. L. Rigaud, L. Letellier, FhuA, an Escherichia coli outer membrane protein with a dual function of transporter and channel which mediates the transport of phage DNA, Biochimie 80 (1998) 363–369, https://doi.org/10.1016/s0300-9084(00)80004-8.

[76] B.C.H. Chu, H.J. Vogel, A structural and functional analysis of type III periplasmic and substrate binding proteins: their role in bacterial siderophore and heme transport, Biol. Chem. 392 (2011) 39–52, https://doi.org/10.1515/BC.2011.012.

[77] R. Burkhardt, V. Braun, Nucleotide sequence of the fhuC and fhuD genes involved in iron (III) hydroxamate transport: domains in FhuC homologous to ATP-binding proteins, Mol. Gen. Genet. 209 (1987) 49–55, https://doi.org/10.1007/BF00329835.

[78] A. Mademidis, H. Killmann, W. Kraas, I. Flechsler, G. Jung, V. Braun, ATP-dependent ferric hydroxamate transport system in Escherichia coli: periplasmic FhuD interacts with a periplasmic and with a transmembrane/cytoplasmic region of the integral membrane protein FhuB, as revealed by competitive peptide mapping, Mol. Microbiol. 26 (1997) 1109–1123, https://doi.org/10.1046/j.1365-2958.1997.6592008.x.

[79] J.W. Coulton, P. Mason, D.D. Allatt, fhuC and fhuD genes for iron (III)-ferrichrome transport into Escherichia coli K-12, J. Bacteriol. 169 (1987) 3844–3849, https://doi.org/10.1128/jb.169.8.3844-3849.1987.

[80] H.K. Chahal, Y. Dai, A. Saini, C. Ayala-Castro, F.W. Outten, The SufBCD Fe-S scaffold complex interacts with SufA for Fe-S cluster transfer, Biochemistry 48 (2009) 10644–10653, https://doi.org/10.1021/bi901518y.

[81] T. Tian, H. He, X.-Q. Liu, The SufBCD protein complex is the scaffold for iron-sulfur cluster assembly in thermus thermophiles HB8, Biochem Biophys. Res. Commun. 443 (2014) 376–381, https://doi.org/10.1016/j.bbrc.2013.11.131.

[82] K. Esquilin-Lebron, S. Dubrac, F. Barras, J.M. Boyd, Bacterial approaches for assembling iron-sulfur proteins, mBio 12 (2021), e0242521, https://doi.org/10.1128/mBio.02425-21.

[83] N. Yokoyama, C. Nonaka, Y. Ohashi, M. Shioda, T. Terahata, W. Chen, K. Sakamoto, C. Maruyama, T. Saito, E. Yuda, N. Tanaka, T. Fujishiro, T. Kuzuyama, K. Asai, Y. Takahashi, Distinct roles for U-type proteins in iron-sulfur cluster biosynthesis revealed by genetic analysis of the Bacillus subtilis sufCDSUB operon, Mol. Microbiol. 107 (2018) 688–703, https://doi.org/10.1111/mmi.13907.

[84] E.I. Corless, E.L. Mettert, P.J. Kiley, E. Antony, Elevated expression of a functional suf pathway in Escherichia coli BL21(DE3) enhances recombinant production of an iron-sulfur cluster-containing protein, e00496-19, J. Bacteriol. 202 (2020), https://doi.org/10.1128/JB.00496-19.

[85] F. D'Angelo, E. Fernández-Fueyo, P.S. Garcia, H. Shomar, M. Pelosse, R.R. Manuel, F. Büke, S. Liu, N. van den Broek, N. Duraffourg, C. de Ram, M. Pabst, E. Bouveret, S. Gribaldo, B. Py, S. Ollagnier de Choudens, F. Barras, G. Bokinsky, Cellular assays identify barriers impeding iron-sulfur enzyme activity in a non-native prokaryotic host, e70936, Elife 11 (2022), https://doi.org/10.7554/eLife.70936.

[86] G.P. Riboldi, H. Verli, J. Frazzon, Structural studies of the Enterococcus faecalis SufU [Fe-S] cluster protein, BMC Biochem. 10 (2009), 3, https://doi.org/10.1186/1471-2091-10-3.

[87] K. Hirabayashi, E. Yuda, N. Tanaka, S. Katayama, K. Iwasaki, T. Matsumoto, G. Kurisu, F.W. Outten, K. Fukuyama, Y. Takahashi, K. Wada, Functional dynamics revealed by the structure of the SufBCD complex, a novel ATP-binding cassette (ABC) protein that serves as a scaffold for iron-sulfur cluster biogenesis, J. Biol. Chem. 290 (2015) 29717–29731, https://doi.org/10.1074/jbc.M115.680934.

[88] K. Dong, S. Wu, B. Chang, T. Sun, Zero-valent iron supported by dendritic mesoporous silica nanoparticles to purify dye wastewater, J. Environ. Chem. Eng. 11 (2023), 110434, https://doi.org/10.1016/j.jece.2023.110434.

[89] T.A. Aragaw, F.M. Bogale, B.A. Aragaw, Iron-based nanoparticles in wastewater treatment: a review on synthesis methods, applications, and removal mechanisms, J. Saudi Chem. Soc. 25 (2021), 101280, https://doi.org/10.1016/j.jscs.2021.101280.

[90] S. Rajendran, S.G. Wanale, A. Gacem, V.K. Yadav, I.A. Ahmed, J.S. Algethami, S. D. Kakodiya, T. Modi, A.M. Alsuhaibani, K.K. Yadav, S. Cavalu, Nanostructured iron oxides: structural, optical, magnetic, and adsorption characteristics for cleaning industrial effluents, Crystals 13 (2023) 472, https://doi.org/10.3390/cryst13030472.

[91] V.K. Yadav, A. Amari, A. Gacem, N. Elboughdiri, L.B. Eltayeb, M.H. Fulekar, Treatment of fly-ash-contaminated wastewater loaded with heavy metals by using fly-ash-synthesized iron oxide nanoparticles, Water 15 (2023) 908, https://doi.org/10.3390/w15050908.

[92] J. Hurtado-Gallego, G. Pulido-Reyes, M. González-Pleiter, G. Salas, F. Leganés, R. Rosal, F. Fernández-Piñas, Toxicity of superparamagnetic iron oxide nanoparticles to the microalga Chlamydomonas reinhardtii, Chemosphere 238 (2020), 124562, https://doi.org/10.1016/j.chemosphere.2019.124562.

[93] N. Hoffmann, G. Tortella, E. Hermosilla, P. Fincheira, M.C. Diez, I.M. Lourenço, A. B. Seabra, O. Rubilar, Comparative toxicity assessment of eco-friendly synthesized superparamagnetic iron oxide nanoparticles (SPIONs) in plants and aquatic model organisms, Minerals 12 (2022) 451, https://doi.org/10.3390/min12040451.